

Pressure strengthening: A way to multimegabar static pressures

Niels E. Christensen

Institute of Physics and Astronomy, Aarhus University DK-8000, Aarhus, Denmark

Arthur L. Ruoff

Department of Materials Science and Engineering, Cornell University, Ithaca, New York 14853

C. O. Rodriguez

Instituto de Fisica de Liquidos y Sistema Biologica, Grupo de Fisica del Solido, C.C. 565, La Plata, Argentina

(Received 1 June 1995)

This paper shows why a static pressure of several megabars can be reached in a diamond anvil cell using a molybdenum gasket whose yield strength at $P=0$ is only 0.04 Mbars. The elastic constants of bcc Mo at 0 K vs reduced volume and pressure were obtained from first-principle, all-electron, density-functional calculations to $V/V_0=0.4$ ($P=11.6$ Mbars) although the fcc phase was calculated to be more stable above 6 Mbars. These constants were used to obtain the Chua and Ruoff pressure scaling factor for the yield strength which combined with plasticity theory shows that a gasket of $2.6 \mu\text{m}$ final thickness can support 6 Mbars.

INTRODUCTION

There have been many calculations of the total energy versus volume for a given crystal enabling the calculation of the bulk modulus versus pressure (or the equation of state) and allowing comparisons of enthalpies of different phases as a function of pressure (and hence phase equilibrium at the absolute zero of temperature). Such calculations on molybdenum have been recently reviewed, with the conclusions that there should be an equilibrium phase transition from bcc to hcp (fcc) in the neighborhood of 5 Mbars.¹ Static pressures of 4.16 Mbars (Ref. 2) and 5.6 Mbars (Ref. 3) have been obtained in molybdenum using molybdenum as the gasket materials in the diamond anvil cell (DAC). Considerably fewer detailed calculations exist for the pressure dependence of the shear constants. We have made thorough calculations of the pressure dependence of the shear constants $C'=(C_{11}-C_{12})/2$ and C_{44} and the bulk modulus B for bcc molybdenum to a reduced volume of $V/V_0=0.40$, which, it is calculated, corresponds to a pressure of 11.6 Mbars (were the bcc phase to persist). These results are used with the variational method of Hashin and Shtrikman⁴ to compute the shear modulus $G(P)$ and the Poisson ratio $\nu(P)$ of the randomly oriented polycrystalline aggregate. Then, using the Chua and Ruoff scaling law⁵ for the yield stress, pressure profiles were computed for the DAC.

CALCULATION OF SINGLE-CRYSTAL ELASTIC CONSTANTS

The density-functional theory⁶ has been used in numerous theoretical calculations of structural and dynamical properties of solids from first principles. Even the crudest approximation, the local-density approximation (LDA), has proven to yield very accurate results in many cases. We also used the LDA for the study of the

elastic properties of Mo under pressure described here. The parametrization by von Barth and Hedin⁷ was chosen, and the self-consistent solution of the one-electron equation was performed by means of the linear muffin-tin-orbital (LMTO) method.⁸ It was shown⁹ that calculation of the elastic shear constants requires the inclusion of the nonspherical parts of the charge densities. The calculations reported here were not based on the "extended force theorem,"⁹ but we used the self-consistent total energy obtained by the full-potential (FP) LMTO method as implemented by Methfessel.¹⁰

Molybdenum assumes the body-centered cubic (bcc) structure at ambient pressure where the (experimental) lattice constant is 5.962 bohrs. The FP-LMTO calculations were performed for volumes ranging from a 15% expansion down to $0.40 V_0$, V_0 being the zero-pressure volume. Some states which at zero pressure are corelike form at the very reduced volumes rather broad bands. For the sake of numerical continuity of the calculated energy versus volume relations, we used, at all volumes, the same grouping into "core" and "valence" electrons, and all calculations were performed in two energy panels. We considered 14 electrons as "valence" electrons. Also, eight electrons ($4s, 4p$) were treated as band forming in a lower-energy panel, whereas six ($4d, 5s, 5p$) were included in the upper panel. The remaining electrons were considered as belonging to a core, but their wave functions were relaxed, i.e., recalculated in each iteration. Three sets of envelope functions were used, a "triple- κ " basis set. Their formal kinetic energies were chosen to be -0.21 , -1.0 , and -2.3 Ry, respectively. The maximum angular momenta included in the basis for these were 3 ($spdf$), 3 ($spdf$), and 2 ($spdf$), i.e., 41 functions per atom.

Reciprocal-space integrations were done by means of special points in the lower panel, whereas the tetrahedron method was used in the upper panel. We applied the lat-

TABLE I. Calculated fractional volume and pressure (Mbars) dependence of the elastic constants of bcc molybdenum (Mbars). Here $C' = (C_{11} - C_{12})/2$.

V/V_0	P	B	C'	C_{44}
1.00	-0.095	2.5819	1.5231	1.0234
0.95	0.0518	3.1631	1.7198	1.2376
0.90	0.2411	3.8545	1.9295	1.4735
0.85	0.4845	4.6784	2.1615	1.7580
0.80	0.7974	5.6612	2.4225	2.0937
0.75	1.1999	6.8360	2.7074	2.4697
0.70	1.7192	8.2486	3.0042	2.9999
0.65	2.3920	9.9447	3.3686	3.6232
0.60	3.2694	12.027	3.6561	4.4450
0.55	4.4274	14.6661	3.9484	5.4601
0.50	5.9890	18.2595	4.0655	6.8062
0.45	8.1874	23.8712	3.8687	8.6571
0.40	11.5669	34.6684	3.0765	11.2082

est version,¹¹ and the necessary integration accuracy was obtained by using more than 1300 irreducible k points.

For each of 15 volumes in the range mentioned above, the total energy was calculated for five tetragonal and five trigonal volume-conserving distortions. Polynomial least-squares fits of the energy versus strain parameter then allowed derivation of the tetragonal and trigonal shear constants as functions of volume. The theoretical pressure-volume (P - V) relation was obtained from the volume derivative of the energy-versus-volume (E - V) curve obtained by fitting a suitable series of functions to the energies obtained for the undistorted crystal. This also yielded the bulk modulus B as a function of volume. Table I gives the calculated volume-pressure dependence of the elastic coefficients. Here V_0 is the experimental value of the volume at 0 K. The corresponding experimental values at $V/V_0=1$ are in Mbars, at 73 K, $B=2.618$, $(C_{11}-C_{12})/2=1.584$, and $C_{44}=1.109$,¹² and at 77 K $B=2.702$, $(C_{11}-C_{12})/2=1.566$, and $C_{44}=1.085$.¹³ These should be less than 0.3% smaller than in the $T=0$ K case. The calculated pressure derivatives at zero pressure are $dB/dP=3.96$, $dC'/dP=1.34$, and $dC_{44}/dP=1.46$. These compare with the experimental values of $dB/dP=4.44$, $dC'/dP=1.48$, and $dC_{44}/dP=1.40$.¹⁴ At 5 Mbars the calculated dB/dP has dropped from 4.0 to 2.3, not far from the free-electron gas value, $\frac{5}{3}$. At higher pressures C' decreases with pressure and, since $B=C_{11}-\frac{4}{3}C'$, B then increases more rapidly. Similar calculations were performed for Mo in the fcc phase.

PHASE STABILITY

The stability of the bcc phase of Mo at high pressures was examined by comparing its theoretical total energy to those of other structures. We chose to consider the fcc, hcp, and ω titanium phases (see, for example, Ref. 15). The calculated E - V and P - V relations were used to deduce the enthalpy of each phase as a function of pressure as shown in Fig. 1, where the bcc values have been

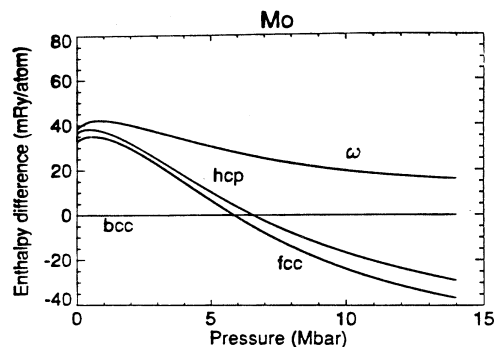


FIG. 1. Calculated enthalpies of bcc, fcc, hcp, and ω -titanium phases of Mo versus (theoretical) pressure. The bcc values have been subtracted to facilitate the determination of the transition pressure.

subtracted. It is seen that the fcc structure is, among those selected here, the most stable for pressures above 6 Mbars. In the case of W we¹⁶ also examined the dhcp structure, and found that this has enthalpy values that are very close to those of fcc W, probably slightly below at high pressures. The results for the hexagonal phases, hcp and ω , included in Fig. 2, were obtained from calculations where the c/a ratios were kept fixed at the respective ideal values, 1.633 and 0.612. Optimization of c/a does not alter the conclusions drawn from Fig. 2 since additional total-energy calculations have shown that the theoretical c/a ratios in both cases vary from 0.95 to 1.00 times the ideal values when the pressure is increased. For pressures above the transition the optimized c/a is identical to the ideal one.

COMPUTATION OF G AND ν

The method of Hashin and Shtrikman⁴ was used to compute upper and lower bounds for G and, since these were quite close, the average was taken as the value for G . The graph of $G(P)$ and $\nu(P)$ are shown in Fig. 2,

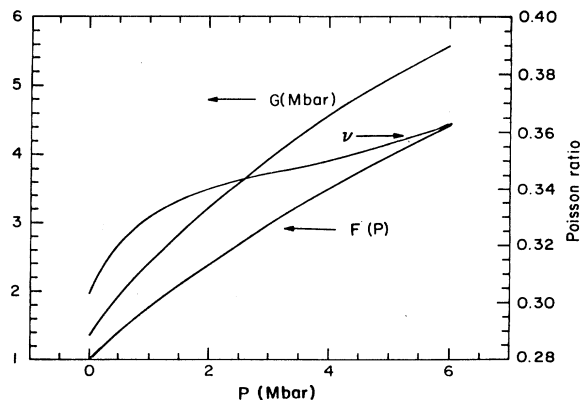


FIG. 2. Calculated bulk shear modulus G and Poisson's ratio ν of molybdenum versus pressure. Also shown is pressure-strengthening scaling factor $F(P)$ increasing by a factor of 4.53.

where $\nu(P)$ is computed from B and G . Chua and Ruoff⁵ give both theoretical reasons and experimental evidence to the effect that the compressive yield stress $\sigma_0(P)$ scales with pressure according to

$$\sigma_0(P)/\sigma_{00}=[G(1-\nu_0)/G_0(1-\nu)]=F(P), \quad (1)$$

where σ_{00} , G_0 , and ν_0 are the corresponding values at zero pressure. Figure 2 shows the scaling factor F versus P . Note that at $P=6$ Mbars $F=4.53$, i.e., the yield strength of molybdenum is 4.53 times larger than at zero pressure (ignoring the additional increase expected due to strain hardening). This is pressure strengthening.¹⁷

CALCULATION OF PRESSURE PROFILES

If we consider a gasket between two anvils with circular tips and parallel faces a distance h apart, it can be shown that the pressure gradient is given by^{3,18}

$$dP/dr = -\sigma_0/h = -\sigma_{00}F(P)/h. \quad (2)$$

This simple plasticity equation closely describes the experimental results for deformation of pure aluminum between sapphire anvils when $F(P)=1$.¹⁹ From Eq. (3)

$$\int_0^P dP/F(P) = -\sigma_{00} \int_a^r dr/h = \sigma_{00}(a-r)/h. \quad (3)$$

At $r=0$, $P=P_{\max}$. We choose to consider the case where $P_{\max}=6$ Mbars; then the integral on the left side equals 2.62. The yield strength for hot-formed molybdenum is 0.021 Mbars and for heavily cold-worked molybdenum is in the neighborhood of 0.063 Mbars.² The gasket is reduced from a thickness of 200 μm to only about 3 μm at room temperature in the DAC. While this rather severe cold working could be expected to strain-harden the gasket to a value nearer the upper limit given, we chose a conservative value of $\sigma_0=0.04$ Mbars. In our diamond anvil cells, $a=150$ μm . Thus, using Eq. (3) with $P=6$ and $r=150$, we obtain $h=2.62$ μm . With h known we can use Eq. (2) to obtain $P(r)$. The results are shown in Fig. 3. It is this pressure strengthening factor along with the high yield strength of heavily strain-hardened Mo at atmospheric pressure which enabled experimentalists to obtain pressures of 5.6 Mbars.³

Also shown by the dashed lines are the slopes at $r=a$ and at $r=0$. The dashed-dotted line passing through $r=a$ gives the pressure profile which would be attained if there were no pressure-strengthening of the gasket. The dashed line passing through $r=0$ has a slope equal to the pressure gradient at $r=0$. The actual steep gradient near to $r=0$, expected from pressure strengthening, makes pressure measurement by the x-ray marker method difficult because it involves an x-ray beam of a finite diameter. Thus experimental profiles will appear rounded at the top²⁰ while actually increasing at nearly an exponential rate. The large pressure present would deform the diamonds so the surface would have to be contoured properly initially for the diamond surface to be flat when $P_{\max}=6$ Mbars is reached. When still further load is applied the diamonds become cupped, i.e., h would be smaller at $r=a$ than at $r=0$. If we assume that Eq. (1) approximately applies when h varies with r , there is one case which we can easily solve. We define H as a function

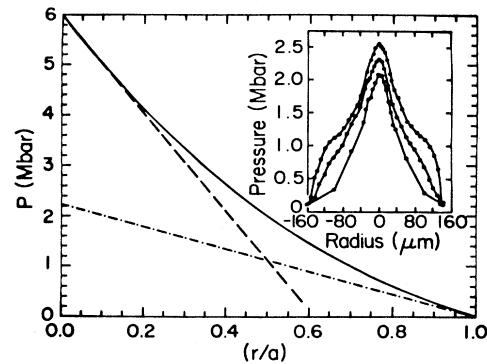


FIG. 3. Computed pressure profile in a diamond anvil cell with a molybdenum gasket, with, in the final state, parallel faces 2.62 μm apart with a face diameter of 300 μm . Inset: Experimental pressure profiles from Ref. 21.

of $1-r/a$ as the ratio of h as a function of $1-r/a$ divided by h at $r=a$. If H versus $1-r/a$ is identical to F versus P/P_{\max} , then

$$P = \sigma_0 a (1-r/a)/h \quad (r=a), \quad (4)$$

i.e., P versus r/a will be a straight line. With the same parameters as before, for $P_{\max}=6$ Mbars we require $h(r=a)=1$ μm in which case $F(6 \text{ Mbars})=4.53$ and $h(r=0)=4.53$ μm . What is done experimentally to contour the diamond anvil is to shape the 16-sided culet with the diameter of 300 μm with a center flat as small as 20 μm and a bevel of, perhaps, 8° from the 16-sided center flat out to the culet perimeter.²

It is of interest to consider an earlier experiment in which beveled anvils were used and the pressure profile was measured, although this involved rhenium rather than molybdenum.²¹ By observing the reflection of light from the culet we could tell when the bevel had flattened (when the maximum pressure was about 2 Mbars). This corresponds to the bottom profile in the inset of Fig. 3. This has the form of the present Fig. 3. The effect of a small h is that the pressure gradient will be very large. When the diamonds become cupped in such a way that H versus $1-r/a$ is identical to F versus P/P_{\max} , then we can expect a linear $P(r)$ profile and this is approximated by the middle profile in the inset of Fig. 3. At still higher loading, further cupping occurs and $h(r=a)$ becomes very small so [see Eq. (2)] the pressure gradient will become large near the perimeter of the culet. Although Eq. (2) is now only a rough approximation when h varies with r , the salient features are still illustrated, with the $h(r)$ term dominating near $r=a$ (leading to a very high gradient) and with the $F(P)$ term very important near $r=0$ (leading to a very high gradient) as shown in the top curve in the inset of Fig. 3 (again the rounding at the top is due to the finite beam size). Detailed calculations involving elastic-plastic behavior of the gasket and non-linear elastic behavior of the diamond using a supercomputer are under way and we hope that we will be able to quantitatively describe the behavior when h varies with r .

While the possible phase transition in Mo may preclude reaching higher pressures with it as a gasket (the

fcc may be weaker; dislocations may be annihilated at the transition) calculations show that B , G , ν , and the volume are only slightly changed at the transition. Other strong materials, such as rhenium, which is hcp and so should strain harden rapidly, might suffice as gasket materials to 1 TPa. Since the diamond anvil also undergoes pressure strengthening,¹⁷ it is conceivable that with proper anvil design a pressure of 1 TPa may be attained.

ACKNOWLEDGMENTS

We acknowledge the support of this work by the Commission of the European Union, Contract No. CII*CT92-0086, the Danish Natural Science Research Council, Contract No. 11-9001-3, and the National Science Foundation under Grant No. MSS 9301443.

-
- ¹P. Söderlund, R. Ahuja, O. Eriksson, and B. Johansson, *Phys. Rev. B* **49**, 9365 (1994).
- ²A. L. Ruoff, H. Xia, H. Luo, and Y. K. Vohra, *Rev. Sci. Instrum.* **61**, 3830 (1990).
- ³A. L. Ruoff, H. Xia, and Q. Xia, *Rev. Sci. Instrum.* **63**, 4342 (1992).
- ⁴Z. Hashin and S. Shtrikman, *J. Mech. Phys. Solids* **10**, 343 (1962).
- ⁵J. O. Chua and A. L. Ruoff, *J. Appl. Phys.* **46**, 4659 (1975).
- ⁶P. Hohenberg and W. Kohn, *Phys. Rev.* **136**, B964 (1964); W. Kohn and L. J. Sham, *Phys. Rev.* **140**, A1133 (1965); L. J. Sham and W. Kohn, *Phys. Rev. B* **145**, 561 (1966).
- ⁷U. von Barth and L. Hedin, *J. Phys. C* **5**, 1629 (1972).
- ⁸O. K. Andersen, *Phys. Rev. B* **12**, 3060 (1975).
- ⁹N. E. Christensen, *Solid State Commun.* **49**, 701 (1983); *Phys. Rev. B* **29**, 5547 (1984).
- ¹⁰M. Methfessel, *Phys. Rev. B* **38**, 1537 (1988); M. Methfessel, C. O. Rodriguez, and O. K. Andersen, *ibid.* **40**, 2009 (1989).
- ¹¹P. Bloechl, O. Jepsen, and O. K. Andersen, *Phys. Rev. B* **49**, 16 223 (1994), and references therein.
- ¹²J. M. Dickinson and P. E. Armstrong, *J. Appl. Phys.* **38**, 602 (1967).
- ¹³D. I. Bolef and J. de Klerk, *J. Appl. Phys.* **33**, 2311 (1962).
- ¹⁴K. W. Katahara, M. H. Manghnani, and E. S. Fisher, *J. Phys. F* **9**, 773 (1979).
- ¹⁵K.-M. Ho, C.-L. Fu, and B. N. Harmon, *Phys. Rev. B* **29**, 1575 (1984).
- ¹⁶A. L. Ruoff, N. E. Christensen, and C. O. Rodriguez (unpublished).
- ¹⁷A. L. Ruoff and H. Luo, *J. Appl. Phys.* **70**, 2066 (1991).
- ¹⁸W. F. Hosford and R. M. Caddell, *Metal Forming Mechanics and Metallurgy* (Prentice-Hall, Englewood Cliffs, NJ, 1983).
- ¹⁹K. S. Chan, T. L. Huang, T. A. Grzybowski, T. J. Whetten, and A. L. Ruoff, *J. Appl. Phys.* **53**, 6607 (1982).
- ²⁰K. E. Brister, Y. K. Vohra, and A. L. Ruoff, *Rev. Sci. Instrum.* **59**, 318 (1988).
- ²¹Y. K. Vohra, S. J. Duclos, K. E. Brister, and A. L. Ruoff, *Phys. Rev. Lett.* **61**, 574 (1988).